Photoswitchable Gas Permeation Membranes Based on Liquid Crystals

Introduction

Research in the field of high-performance gas permeation membranes has, to date, focused on maximizing both mass transfer and selectivity. Although gateable interconnect membranes for liquids have evolved to a mature level, the development of gas membranes whose permeability can be controlled during operation or tuned to respond to changes in their environment is an important goal that has yet to be realized.[1,2] Such "smart" materials are in high demand for smaller-scale membrane applications such as microanalysis, reactor devices, and also larger batch processes.[2] Our goal was to create a novel and scaleable membrane system to achieve complex chemical and fluidic manipulations controllable by external stimuli.

Our inspiration for employing liquid crystal materials as the "active" element for switchable and tunable gas separation membranes comes from two sources: (1) biological membranes composed of various types of lyotropic liquid crystal phospholipids, which, because of their enhanced ordering, make it possible to control reversible structural modifications and corresponding permeation changes, and (2) synthetic polymer-based membranes, where the sorption–diffusion process is controlled by segmental mobility and the free volume of the material. Primary relaxation processes of polymers, such as the glass transition, correspond to large changes in sorption–diffusion characteristics.[3]

Mesogenic materials offer a range of thermotropic secondary transitions that can potentially afford unique and tunable materials for permeation membranes. In the early 1980s Kajiyama and co-workers were the first to exploit these properties of mesogenic materials in a series of polymer-dispersed liquid crystal (PDLC) membranes. Such a system has many of the advantages of a liquid-diffusing phase, such as high mobility of permeants, yet retains the mechanical properties of a polymeric material. LC–polymer composites have been exploited for light-controlled active transport of metal ions; however, the majority of efforts have focused on harnessing thermotropic control. These PDLC systems demonstrated significant deviations in their permeation properties at both the crystalline–nematic and the nematic–isotropic transition temperatures.[4] An obvious caveat is that using changes in temperature to vary the permeability of the membrane material is intrinsically coupled to the kinetics of the permeant. Employing thermal events to tune permeability can be not only energy intensive but for many applications may also have an unacceptably long response time because of unfavorable thermal transport characteristics of polymer materials. Although thermally induced LC phase changes have been successful for controlling permeation in drug delivery applications,[5] the primary aim of this work was to avoid the complications mentioned above by evaluating the permeation characteristics of LC materials under isothermal conditions.

To generate phase changes isothermally, a technique was adopted that is well established in LC photonics—using photochromic dyes that demonstrate a photomechanical effect. Azobenzene derivatives are among the most-studied and frequently employed photochromic dyes that convert incident light to mechanical energy through the process of *trans-cis* isomerization. Appropriate substitution at the *para* positions affords azobenzene derivatives, where the *trans* form is mesogenic because of its rod-like shape. In contrast, the *cis* isomer's bent shape substantially perturbs LC ordering. This effect is illustrated in Fig. 122.1.

Several demonstrations of bulk nematic- to isotropic-phase changes induced by *trans-cis* photoisomerization in azobenzenes have been conducted in both low-molar-mass and polymeric systems. This "photomechanical" effect has been exploited to generate numerous types of reversible changes when azobenzene materials are added as "guest" dopants to both fluid and polymer "hosts." Several extensive reviews document the azobenzene photomechanical effect in bulk materials.[6]

For efficient photoswitching in LC-based permeation membranes, the concentration of azobenzene absorbers in the LC host must be carefully selected to be large enough to effectively induce an isothermal phase shift but not large enough to pre-

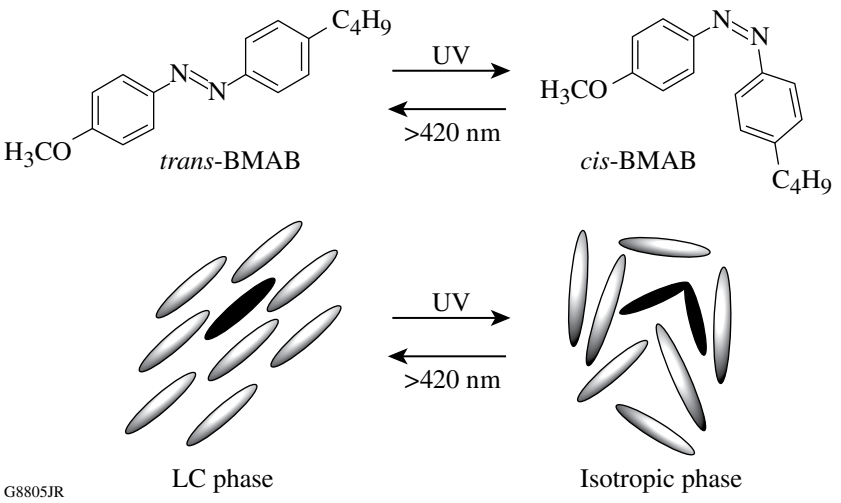

Figure 122.1
Photomechanical effect of 4-butyl-4′-methoxyazobenzene (BMAB) utilized to afford reversible isothermal LC-isotropic phase transitions.

vent penetration of the activating optical radiation throughout the bulk of the film. The particularly high molar extinction coefficient of azobenzenes makes it especially important to limit their content in the membranes to ensure that the entire depth of the film is actuated. Two azo-containing eutectic LC mixtures were prepared (Fig. 122.2). The azobenzene dye 4-butyl-4′-methoxyazobenzene (BMAB) has been used extensively as a photoresponsive mesogenic chromophore to generate refractive-index changes in thin polymer films[7] and for optical data storage;[8] it has also been incorporated at 15 wt% in a eutectic mixture with Merck E7 for photoswitching between the nematic and isotropic phases.[8]

To study the influence of chemical composition on permeation, a second eutectic mixture (Eutectic 2) based on the phenyl benzoate LC materials 4-pentyl-4′-methoxybenzoate (PPMeOB) and 4-pentyl-4′-pentoxybenzoate (PPPOB) was used along with 4-ethoxy-4′-hexanoylazobenzene (EHAB) as the azobenzene dopant. Because both Eutectic 1 and Eutectic 2 have similar nematic ranges, viscosities, and dye content, these systems represented a nearly ideal "matched set" for evaluating the relationship of chemical composition of the LC phase on gas permeability in the confined membrane environment.

Photoswitchable membranes were fabricated either by dispersing the azobenzene-doped LC eutectic mixture into a host polymer solution and casting as a PDLC membrane as described by Kajiyama *et al.*[7] or by imbibing the LC material directly into the cylindrical "track-etched" micropores of a commercial polycarbonate (Isopore) membrane. Isopore mem-

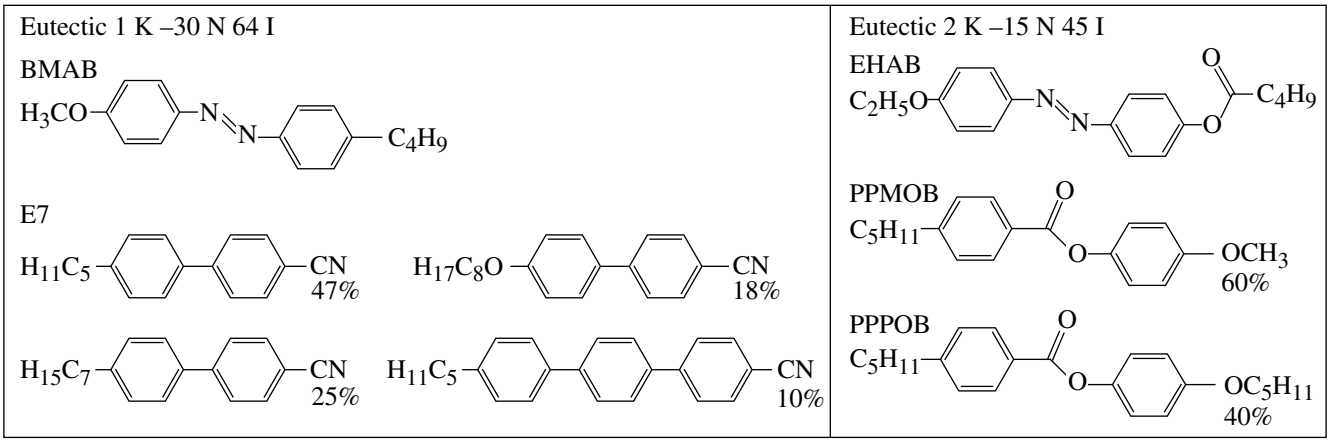

Figure 122.2
Molecular compositions and thermal properties of the two LC mixtures used.

branes are formed by bombardment with high-speed alpha particles, followed by chemically etching the damaged radiation tracks to produce cylindrical pores with remarkably smooth cavity surfaces. Previous studies of nematic LC materials confined in such a micropore environment have shown that the pore walls function as a homogenous alignment surface, resulting in the nematic director field configuration being uniaxial and parallel with respect to the pore wall.[9] To test the effect of the LC alignment state (parallel or perpendicular to the pore walls) on permeation, the pore walls were treated with the reactive silane n-octyltriethoxysilane (OTS). Figure 122.3 shows a schematic diagram of how a photoswitchable LC material imbibed into a porous polymer membrane could be used for gas-phase switching and tuning applications. Using the well-defined, cylindrically symmetrical, preformed porous structure of the membrane makes it possible to directly and conveniently probe the permeation properties of the photoswitchable LC host in the membrane as a function of LC orientation and irradiation. Porous membranes imbibed with LC proved to be much better candidates than PDLC materials. We characterized the optical, thermal, and orientational properties of the confined LC eutectics and evaluated their permeation qualities, along with demonstrating reversible permeation control of nitrogen gas.

Results and Discussion

1. Photocontrollable PDLC Membranes

Our initial attempts focused on creating PDLC's for functional gas permeation membranes in a manner similar to that reported by Kajiyama *et al.*[3] The major challenge in fabricating PDLC membranes for permeation applications is that the

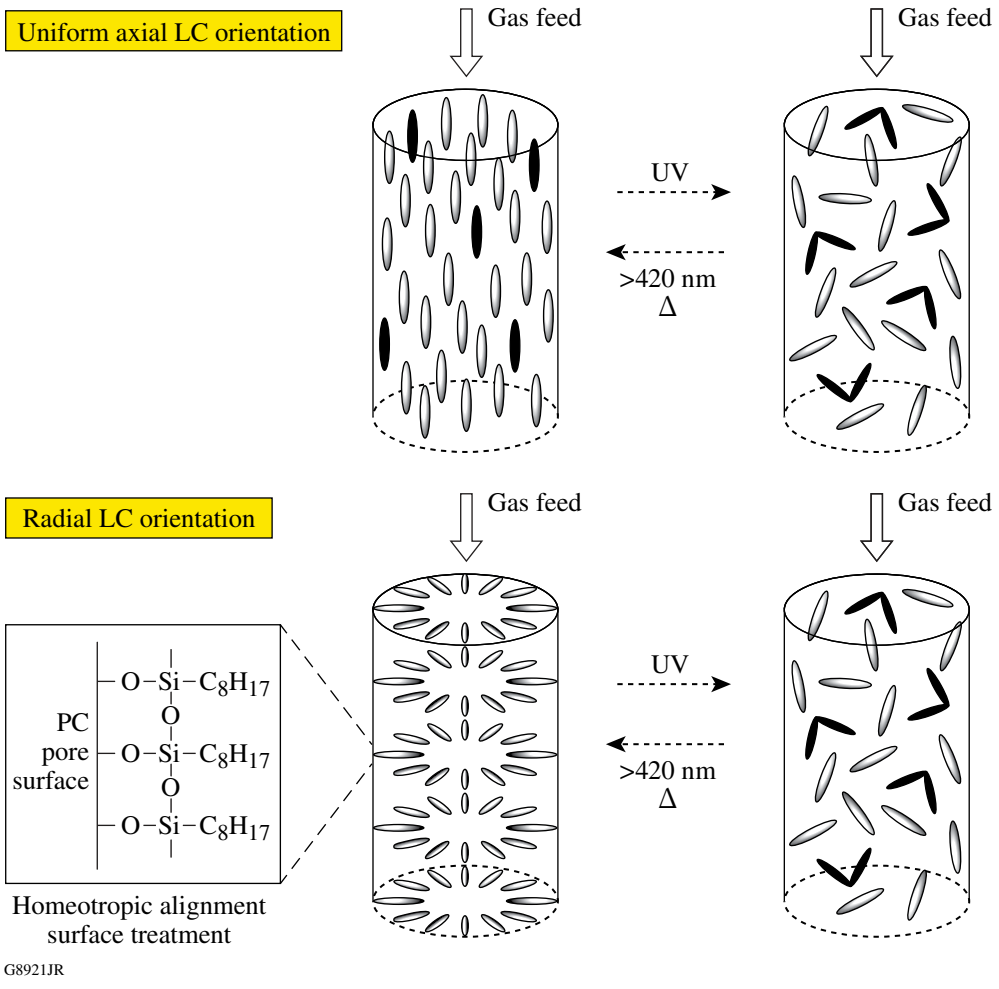

Figure 122.3
Photoswitchable operation of LC/mesogenic dye confined in track-etched pores based on reversible nematic–isotropic phase changes. Both homogeneous and homeotropic (radial) alignments with respect to the confining pore wall are evaluated in this article.

confined LC material will often heavily plasticize the polymer host, producing membranes without the necessary mechanical robustness. The PDLC's reported by Kajiyama overcame this difficulty by using a large thickness (several hundred microns), which precludes efficient photoactuation through the depth of the film because of the high extinction coefficient of azobenzene in the LC mixture. Although we successfully fabricated poly(vinyl chloride) (PVC)-based freestanding membranes that were only a few microns thick, they proved to be insufficiently mechanically robust and were ruptured by pressures >1 psi. Attempts to improve the membrane strength by using poly(methyl methacrylate) (PMMA) crosslinked with ethylene glycol dimethacrylate as the host polymer produced membranes that were extremely mechanically robust. The LC, however, still plasticized the host, resulting in membranes that stretched and "ballooned out" under pressure, but did not break because of the strength of the crosslinked PMMA. Based on these results, it became immediately apparent that, even with a great deal of additional materials research activities, freestanding PDLC membranes would not be practical candidates for photocontrolled membranes in the short term.

2. Photocontrollable Track-Etched Membranes with Imbibed LC Material

a. Photoswitching and kinetics. The relatively thin membrane cross section of the photoswitchable LC-imbibed Isopore polycarbonate membranes (≈10 μm), along with their high transparency in the long-wavelength-range UV, makes reversible photoswitching possible by irradiation through alternating bandpass filters (365 nm or 420 nm).

To demonstrate that photoisomerization was indeed solely responsible for the observed phase changes, UV-Vis spectra were obtained for Isopore films imbibed with Eutectic 1 and Eutectic 2 both before and after irradiation under the same conditions (Fig. 122.4). Ten seconds of irradiation time (which corresponds to a fluence of 2 mW/cm^2) is sufficient to nearly eliminate the absorbance band from the *trans* isomer at ≈360 nm. The accompanying rise of absorption at 420 nm from the photogenerated *cis* isomer appears as a small peak because of the low molar extinction coefficient of the *cis* isomer relative to the *trans* isomer. The 360-nm peak that appears as a shoulder in the spectrum of the Eutectic 1–imbibed membranes is due to the absorbance of the cyanobiphenyl components of the E7 host LC. Irradiation with light >420 nm regenerates the *trans* form and affords the complete return to the original pre-irradiation spectrum for both eutectic mixtures. As is well known from PDLC research, the refractive-index mismatch between micrometer-sized nematic droplets and the polymer host results in a highly scattering film,[10] and this refractive-index mismatch can be changed by inducing the LC material to undergo a phase change to the isotropic state either thermally or photochemically. In the case of an LC host containing azobenzene dyes imbibed in a porous polycarbonate membrane, a similar photochemically induced phase change can be expected. The inset in Fig. 122.4 shows an image viewed through a stack of

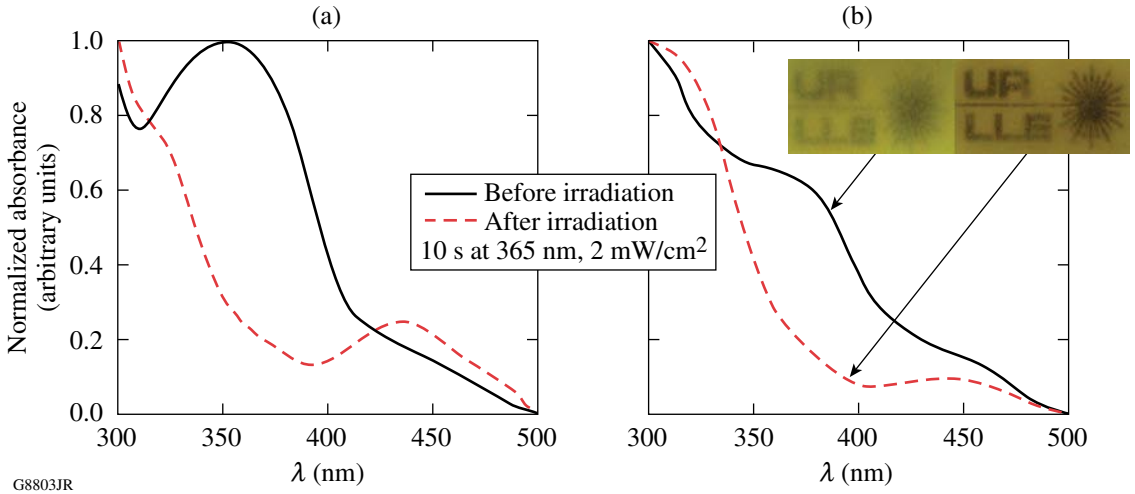

Figure 122.4
UV-Vis spectra of imbibed Isopore membranes before and after irradiation with UV light. Plot (a) shows Eutectic 2, plot (b) Eutectic 1. The inset in the upper right shows three stacked Eutectic 1–imbibed membranes before and after irradiation, demonstrating the narrowing of refractive-index mismatch between host polycarbonate and confined Eutectic 1.

three photoswitchable LC-imbibed polycarbonate membranes containing Eutectic 1 (total path length = 30 μm) before and after irradiation with 365-nm UV. Although the contrast ratio between irradiated and non-irradiated membranes was relatively low because of the small LC domain size (400-nm LC-containing pores) in these membranes, they nevertheless clearly demonstrate that an LC-to-isotropic phase change is indeed occurring under the selected irradiation conditions. The isothermal nematic–isotropic phase changes were also verified by polarized optical microscopy (POM) (see **Dispersion State of Imbibed LC Materials** below).

The kinetics of thermal relaxation of the azobenzene dyes from the photogenerated *cis* state back to the original *trans* state in the confined environment are a parameter of interest. After irradiating a membrane for 10 s at 2 mW/cm^2, the change in absorbance $\left(A_t/A_0\right)$ at 365 nm was monitored as a function of time. The recovery of the *trans* isomer π-π^* absorption band with time obeys first-order kinetics for azobenzene dyes dissolved in solution. Azobenzene chromophores in the solid state, such as in thin films, are known to follow a more-complex behavior. This behavior is due to the fact that steric effects of the host environment on the azo dye affect the thermodynamics of thermal *cis-trans* isomerization. Figure 122.5 shows a logarithmic plot of A_t/A_0 as a function of time. The steep initial rise in the curve followed by a more-gradual leveling off and linear behavior is attributed to a first-order process with two rate constants, with the greater rate constant corresponding to azobenzene *cis* isomers that are in a more-strained environment. Because of the alignment effect of the confining surface,[11] we hypothesize that azobenzene mesogens close to the pore wall isomerize faster than those in the bulk. We found that the thermal relaxation of confined azobenzene mesogens resembled that of azobenzenes in the solid state[11] and could be modeled using the biexponential expression

$$[\text{trans}]_t/[\text{trans}]_0 = \alpha\exp[-k_1 t] + (1-\alpha)\exp[-k_2 t]. \quad (1)$$

The calculated rate constants are an order of magnitude greater than typical azobenzenes in solution in an isotropic solvent.[12] The OTS-aligned Eutectic 1 proved to be anomalous to the other confined materials in that photoinduced isomerization occurred more slowly, and only after 10 min in the dark did the *cis*-isomer population begin to decline. We are currently conducting experiments to explain this observation.

b. Dispersion state of imbibed LC materials. Understanding the ordering of mesogenic molecules in the porous membrane structure is requisite to interpreting the permeation characteristics of such materials. We evaluated the nematic range of the eutectic materials both in the bulk state and imbibed into the pores using both POM and differential scanning calorimetry (DSC). For DSC evaluation, the membranes were carefully chopped into pieces and then packed into a DSC pan for measurement. Although the quantity of mesogenic material in the pores was very small, definite phase-transition endotherms were visible with good signal-to-noise ratio at scan rates ≥40°C/min on both heating and cooling. Repeated cycling produced no noticeable changes in the DSC thermograms for all samples evaluated. Thermograms for the eutectic materials in both the free-bulk and confined geometries were normalized to bal-

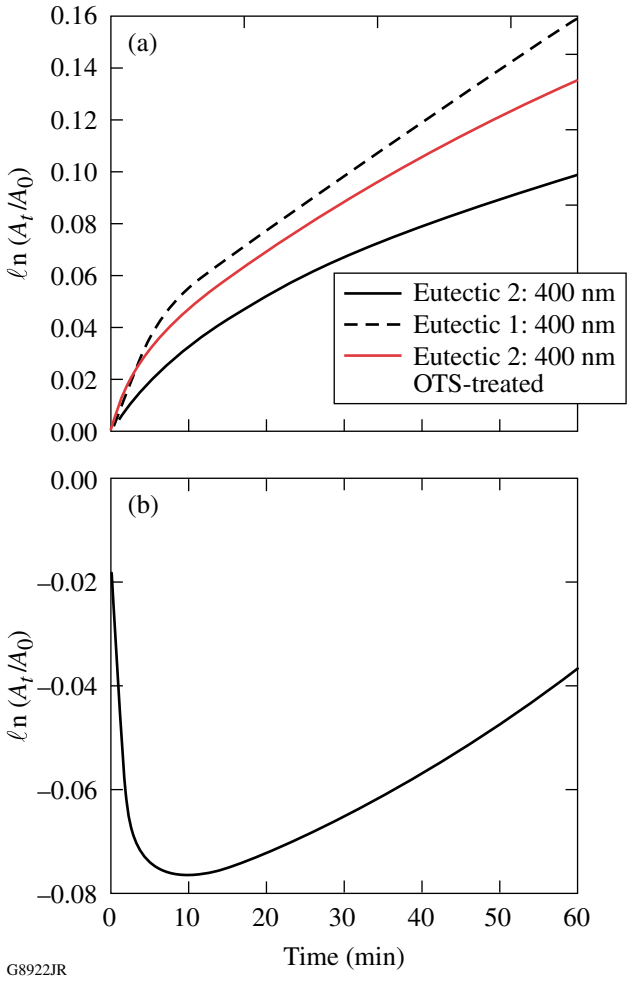

Figure 122.5
Normalized absorption $\left(A_t/A_0\right)$ over time for the two eutectic mixtures at 360 nm following 10 s of irradiation (2 mW/cm^2). Measurements were taken in the dark over 1 h, every 10 s. (a) Unaligned Eutectic 1: $k_1 = 0.72 \times 10^{-2}$ min^{-1}, $k_2 = 0.20 \times 10^{-2}$ min^{-1}. Eutectic 2: $k_1 = 0.61 \times 10^{-2}$ min^{-1}, $k_2 = 0.19 \times 10^{-2}$ min^{-1}. OTS-aligned Eutectic 2: $k_1 = 0.73 \times 10^{-2}$ min^{-1}, $k_2 = k_2 = 0.20 \times 10^{-2}$ min^{-1}. Graph (b) shows the anomalous behavior of OTS-aligned Eutectic 1 in 400-nm pores.

ance out the large disparity in sample quantity. Figure 122.6 compares the nematic–isotropic phase-transition temperatures for the two photoswitchable eutectic mixtures in the free-bulk versus the confined environment of the membrane pores, with and without treatment with OTS. For Eutectic 1 (biphenyl host), the nematic–isotropic transition temperature T_{cl} decreased only slightly in the confined state, while in Eutectic 2 (phenylbenzoate host) T_{cl} increased relative to the bulk material, which indicates the confined environment increases the LC bulk order and stabilizes the LC phase. For the biphenyl host (Eutectic 1), the observed reduction in T_{cl} may be caused by extraction of trace unreacted monomers from the porous polycarbonate membrane since biphenyl materials such as E7 are well known to plasticize many different polymer systems. Studies of E7 (Ref. 13) and other cyanobiphenyl LC materials[12] in PDLC's have also shown very small drops in T_{cl} of dispersed nematic droplets. OTS treatment increased the T_{cl} for both confirmed eutectics, suggesting the effectiveness of this treatment in supporting LC alignment.

Direct observation by POM of the texture of the LC photoswitchable host confined in the 400-nm pores of the Isopore membrane was not possible because of (1) the regions of highly crystalline polycarbonate domains of the order of several microns that extensively scatter light in the membrane and (2) the high birefringence of the membrane imparted by the extrusion process used in its fabrication. For Isopore membranes with 10-μm pores, we were able to easily image the LC orientation in the pores by keeping the optical axis of the film fixed so that it was always aligned parallel to the incident polarizer. Rotating the analyzer so that it was oriented either parallel or perpendicular to the incident polarizer allowed one to see the confined LC at 1000× total magnification using combinations of transmitted and reflective illumination. Prior to imaging the membrane, any remaining traces of free LC material were removed from the surface by spinning the membranes at 3000 rpm and washing with several drops of hexane. Figure 122.7 shows a series of photomicrographs of the two photoswitchable LC eutectics imbibed into 10-μm pores of Isopore membranes. When viewed under crossed polarizers in reflection and transmission, the pores appeared as brighter areas while the surrounding polymer matrix appeared dark. The smeared birefringent areas around some of the pores are most likely caused by leaching of the LC eutectic into defect voids that extend laterally out from any pore walls that have been over-etched during membrane manufacture. Viewing under crossed polarizers with both transmitted and reflected illumination while rotating the sample stage establishes that the LC molecules are uniaxially arranged in the 10-μm pores and parallel to the pore axis. These findings are consistent with the ^{2}H NMR studies of Crawford *et al.*[11] for nematogens in Isopore membrane pores, as well as for inorganic porous photonic

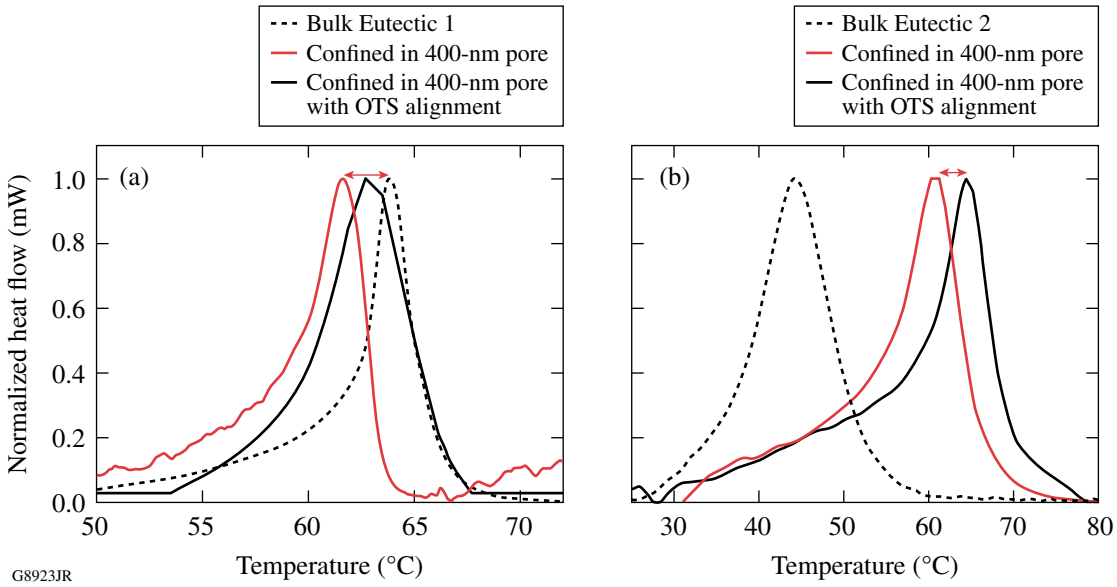

Figure 122.6
DSC heating scans for (a) Eutectic 1 and (b) Eutectic 2. Note that the signals are normalized to compensate for large disparity in sample quantity.

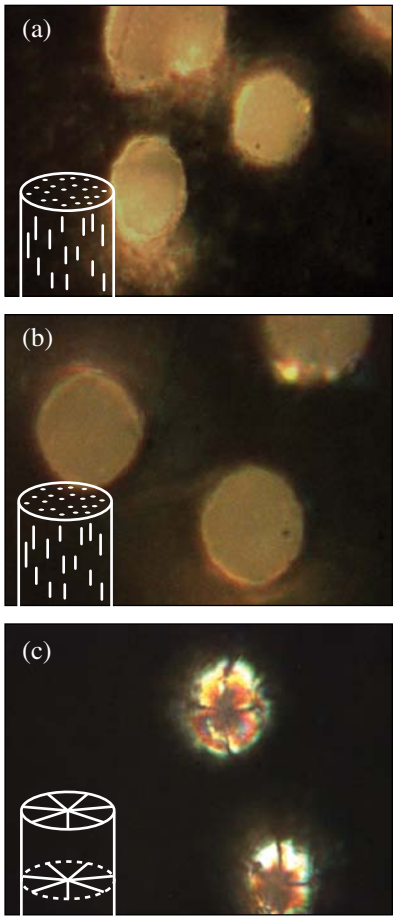

Figure 122.7
POM images of LC material confined in 10-μm pores. (a) Eutectic 1 without alignment, (b) Eutectic 2 without alignment, and (c) Eutectic 1 in a pore treated with 2% OTS solution. The inset drawings illustrate the orientation of the nematic director fields.

crystals (200- to 600-nm pores) imbibed with LC materials.[14] Membranes treated with OTS demonstrated the Maltese-cross optical texture that is characteristic of radial alignment.

c. Permeation properties. Permeation tests are carried out using a traditional volume/time method to determine the steady-state permeation coefficient P (Ref. 15). The coefficient P is defined as the Fickian flux (J) times the value of membrane thickness (l) divided by the pressure difference (Δp) across the membrane, where the flux J equals the concentration gradient (concentration ϕ divided by length x) multiplied by a diffusion coefficient D:

$$J = -D\frac{d\phi}{dx} \tag{2}$$

$$P = \frac{J \cdot l}{\Delta p}. \tag{3}$$

After the membranes equilibrate at a given pressure, the volume of nitrogen diffused over time is measured. The membrane is then irradiated with 365-nm light for 5 s (2 mW/cm^2) to switch it into the isotropic state and subsequently reach equilibrium, after which the permeability is re-measured. Irradiation is then conducted using >420 nm for the same time and intensity as the UV irradiation to photoswitch the membrane back to the LC state. This test cycle is repeated to check for reversibility, which we define as four cycles between the alternately photogenerated states without measurable deviations from steady-state permeation behavior of the respective states. From our initial tests, a clear relationship emerged between confining pore size and the capacity to withstand incident pressure. Membranes with larger pores do not display sufficient stability with respect to sustained irradiation–permeation cycles. Neither 5-μm nor 10-μm pore sizes provided sufficient confinement strength to retain the LC eutectics in the pores. We did find that 400-nm pores perform very well over consecutive test cycles. Imbibed 400-nm pore membranes were 6 to 7 orders of magnitude less permeable than empty membranes. When filled with LC eutectics, they exhibited permeability of the same range as highly permeable rubbery polymeric materials, such as poly(dimethyl siloxane).[1] Both LC materials display good reversibility below 500 mmHg. Figure 122.8 shows permeability versus pressure (P/p) data for Isopore membranes with 400-nm pores imbibed with both Eutectic 1 and Eutectic 2. Both materials appear to follow ideal linear P/p behavior in both the LC and the isotropic states.

The isotropic state provides greatly increased permeation in photoswitched imbibed Eutectic 1. Treatment with OTS slightly lowers the permeability of the photogenerated isotropic state, although that of the LC state is unchanged. We conclude that uniaxial versus radial alignment has no effect on the permeability of Eutectic 1. In the case of Eutectic 2, the photogenerated isotropic state is less permeable than the initial LC state, and overall permeability values are an order of magnitude lower than Eutectic 1. The effect of the OTS alignment is significantly more pronounced. The increased T_{cl} shown by DSC and the faster *cis-trans* thermal isomerization suggest that enhanced LC ordering is responsible for lower permeation. Eutectic 1 shows permeation overall an order of magnitude greater than Eutectic 2, for both LC and isotropic states, with or without OTS treatment. This finding leads us to conclude that the intrinsic sorption–diffusion–desorption properties (with respect to nitrogen) of the imbibed material are what change upon photoirradiation. Increasing the permeation difference

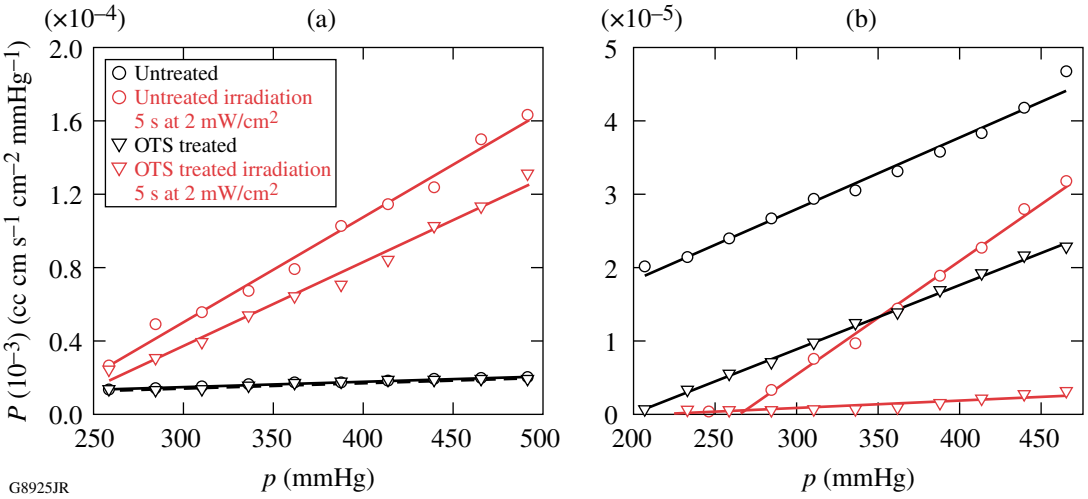

Figure 122.8
Permeability/pressure relationships for imbibed LC materials in 400-nm pores: (a) Eutectic 1 and (b) Eutectic 2. Photoswitching causes a reversible change in the permeation coefficient *P*.

between photogenerated states and achieving potential tunable selectivity are the subjects of our ongoing investigations.

Conclusions

The results of this effort have shown that photoswitchable LC materials based on azobenzene derivatives as the active element have potential for application to reversible photocontrollable gas permeation membranes. The imbibed mesogenic materials offer several tunable variables based on exploiting LC composition and alignment effects. For all imbibed materials, linear sorption–diffusion behavior was observed. Isothermal permeability switching response times between the LC and isotropic state of 5 s were demonstrated at an intensity of 2 mW/cm^2 using alternating UV and >420-nm radiation. Our goal now is to increase the overall differences in permeability that can be achieved through photoswitching, as well as explore possibilities for tunable selective permeation. These goals lead us to focus on exploiting the multitude of LC phases that are regularly used for various electro-optical applications (smectic phases, chiral phases, etc.). These materials potentially offer many types of tunable-ordered media that can be applied to separation technology and gateable interconnects in "smart" photocontrollable membranes.

Experimental

1. Preparation of Photoswitchable LC Mixtures

Photoswitchable eutectic mixtures were prepared by adding an azobenzene LC material to an existing eutectic LC mixture and mixing above the isotropic temperature of the mixture. The phase transition of the mixtures was verified by hot-stage polarizing microscopy (POM). The composition of the two mixtures studied is given in Fig. 122.2. Eutectic 1 was prepared by doping 14% w/w of the azobenzene 4-butyl-4′-methoxyazobenzene (BMAB) into the biphenyl host Merck E7 at an elevated temperature. This azobenzene compound was synthesized, as previously reported.[16] Eutectic 2 was prepared by doping 15% w/w of 4-ethoxy-4′-hexanoylazobenzene (EHAB) obtained from Eastman Chemical into a 60:40 w/w eutectic mixture of 4-pentylphenyl-4′-methoxybenzoate (PPMeOB) and 4-pentylphenyl-4′-pentoxybenzoate (PPPOB) at an elevated temperature. These two phenylbenzoate materials had been previously synthesized and purified in-house using well-known preparation and purification techniques.

2. Preparation of LC-Imbibed Track-Etched Membranes

Track-etched, 10-μm-thick Isopore polycarbonate films (Millipore Corp.) with pore sizes of 0.4 μm, 5 μm, and 10 μm were heated to 100°C in vacuum (200 mtorr) overnight to remove water and other volatile components. The membranes were imbibed with LC through capillary action by completely immersing them into the LC eutectic at a temperature above the LC isotropic transition (80°C) for 1 h. Excess LC on the surfaces of the membrane was removed by carefully rubbing the membranes between two sheets of filter paper. To achieve homeotropic alignment, reactive silane octyl triethoxysilane (OTS) was used. Membranes were immersed in a solution of 2-wt% OTS in ethanol with a few drops of acetic acid catalyst for 5 min, then dried in a vacuum oven. For POM imaging,

all residual LC material was removed from the surface by spinning the membranes at 3000 rpm and washing with a few drops of hexane. Photoswitching experiments were conducted using a Rolence Technologies Q-Lux handheld UV curing unit (365 nm at 70 mW/cm^2). The output wavelength bandwidth was narrowed to 365 nm and 420 nm, as required, using optical bandpass filters (Edmund Optics).

3. Characterization

Differential scanning calorimetry (DSC) measurements were conducted using a Perkin-Elmer DSC 7 with a CCA-7 liquid nitrogen subambient accessory. The sample and reference compartments were purged with nitrogen at a flow rate of 20 ml/min. Optical spectroscopy (UV-VIS) was accomplished using a Perkin-Elmer Lambda 900 spectrophotometer, while visualization of the LC confined in the porous membrane structure was carried out using either a Leitz Orthoplan POL polarizing microscope or a Leica DMRX polarizing microscope at up to 1000× total magnification with reflected and transmitted illumination.

4. Permeability Measurements

The permeability of the photoswitchable LC membranes to nitrogen was measured according to the volume/time method using an apparatus that was constructed in-house. The membrane being tested was clamped between two rubber gaskets in an aluminum manifold and equilibrated with a given upstream pressure (200 to 500 mmHg). The permeation cell was designed in such a way that the membrane was irradiated directly. The permeation area was 0.5 cm^2.

ACKNOWLEDGMENT

This work was supported by the U.S. Department of Energy Office of Inertial Confinement Fusion under Cooperative Agreement No. DE-FC52-08NA28302, the University of Rochester, and the New York State Energy Research and Development Authority. The support of DOE does not constitute an endorsement by DOE of the views expressed in this article.

REFERENCES

1. D. R. Paul and Y. P. Yampol'skii, in *Polymeric Gas Separation Membranes*, edited by D. R. Paul and Y. P. Yampol'skii (CRC Press, Boca Raton, FL, 1994), Chap. 1, pp. 1–17.
2. M. Ulbricht, Polymer **47**, 2217 (2006).
3. T. Kajiyama, in *Polymers for Gas Separation*, edited by N. Toshima (VCH Publishers, New York, 1992), Chap. 3.
4. T. Kajiyama, A. Takahara, and H. Kikuchi, Polym. J. **23**, 347 (1991).
5. R. Dinarvand and M. Ansari, J. Membr. Sci. **223**, 217 (2003).
6. R. H. El Halabieh, O. Mermut, and C. J. Barrett, Pure Appl. Chem. **76**, 1445 (2004); C. J. Barrett *et al*., Soft Mat. **3**, 1249 (2007); G. S. Kumar and D. C. Neckers, Chem. Rev. **89**, 1915 (1989).
7. H. Kurihara, A. Shishido, and T. Ikeda, J. Appl. Phys. **98**, 083510 (2005).
8. T. Ikeda and O. Tsutsumi, Science **268**, 1873 (1995).
9. G. P. Crawford *et al*., J. Chem. Phys. **96**, 7788 (1992).
10. M. R. LaPointe and G. M. Sottile, in *Solar and Switching Materials*, edited by C. M. Lampert, C.-G. Granqvist, and K. L. Lewis (SPIE, Bellingham, WA, 2001), Vol. 4458, pp. 112–119.
11. I. Suzuki *et al*., Macromolecules **35**, 577 (2002); I. Mancheva, I. Zhivakov, and S. Nespurek, J. Optoelectron. Adv. M. **7**, 253 (2005).
12. W. Ahn *et al*., Macromolecules **25**, 5002 (1992).
13. S. R. Challa, S. Q. Wang, and J. L. Koenig, J. Therm. Anal. **45**, 1297 (1995).
14. P. El-Kallassi *et al*., J. Opt. Soc. Am. B **24**, 2165 (2007).
15. D. W. Brubaker and K. Kammermeyer, Anal. Chem. **25**, 424 (1953).
16. E. Głowacki, K. L. Marshall, and C. W. Tang, in *Liquid Crystals XIII*, edited by I. C. Khoo (SPIE, Bellingham, WA, 2009), Vol. 7414, p. 74140H.